BIOCHEMISTRY
including biophysical chemistry & molecular biology

ARTICLE

pubs.acs.org/biochemistry

Dimeric States of Neural- and Epithelial-Cadherins are Distinguished by the Rate of Disassembly

Nagamani Vunnam,[†] Jon Flint,[†] Andrea Balbo,[‡] Peter Schuck,[‡] and Susan Pedigo*[,†]

[†]Department of Chemistry and Biochemistry, University of Mississippi, University, Mississippi 38677

[‡]Dynamics of Macromolecular Assembly LBPS, National Institute of Biomedical Imaging and Bioengineering (NIBIB), National Institutes of Health, Bethesda, Maryland 20892

S Supporting Information

ABSTRACT: Epithelial- and neural-cadherins are specifically localized at synapses in neurons which can change the shape and contact surface on a time scale of seconds to months. We have focused our studies on the role of the extracellular domains of cadherins in the dynamics of synapses. The kinetics of dimer disassembly of the first two extracellular domains of E- and N-cadherin, ECAD12 and NCAD12, were studied with analytical size exclusion chromatography and sedimentation velocity. NCAD12 forms three different dimers that are distinguished by assembly conditions and kinetics of dissociation. ECAD12 dimer disassembles rapidly regardless of the calcium concentration, whereas the disassembly of NCAD12 dimers was strongly dependent on calcium concentration. In addition to the apo- and saturated-dimeric forms of NCAD12, there is a third dimeric form that is a slow exchange dimer. This third dimeric form for NCAD12, formed by decalcification of the calcium-saturated dimer, was kinetically trapped in apo-conditions and did not disassemble over a period of months. Sedimentation velocity experiments showed that this dimer, upon addition of calcium, had similar weighted averages as a calcium-saturated dimer. These studies provide evidence that the kinetics of dimer disassembly of the extracellular domains may be a major contributor to the morphological dynamics of synapses in vivo.

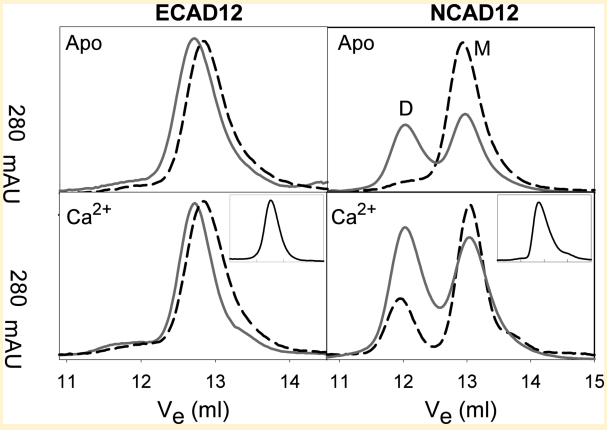

Cadherins are the primary calcium-dependent cell-adhesion molecules in solid tissues. They are involved in several aspects of neural development, including synaptogenesis, synapse maintenance,[1,2] and regulation of synaptic plasticity.[3,4] In the central nervous system, different members of the cadherin family are expressed at specific locations.[5−7] E- and N-cadherins are specifically localized in neurons at two different types of synapses, inhibitory and excitatory, respectively, which have distinctly different calcium signaling properties.[8−10] Excitatory synapses are found at dendritic spines and are known to undergo large fluxes in extracellular calcium concentration.[11] Dendritic spines show heterogeneity in morphology and morphological dynamics in vivo.[12,13] Although other cell adhesion molecules are located at synapses, N-cadherin is considered a "synaptic tag" for actively stimulated excitatory synapses.[14,15] Inhibitory synapses are found at dendritic shafts, soma and proximal axonal regions of neurons.[16−18] At an inhibitory synapse, the concentration of calcium is relatively constant since the signal to release neurotransmitters is due to local perturbation in potassium and chloride ions. Since calcium levels are necessarily different at inhibitory and excitatory synapses, we propose that calcium-dependent differences in the dimerization properties of these two proteins play a role in the dynamics of synapses observed in vivo.

Classical cadherins comprise an extracellular (EC) region that binds calcium, a transmembrane segment, and a conserved C-terminal cytoplasmic region.[19−21] Cell−cell adhesion occurs through the formation of adhesive dimers, which are formed through a strand-crossover interaction between the EC-region of cadherins from neighboring cells.[22,23] Although the cytoplasmic region is necessary for communication with the actin cytoskeleton[24−26] and critical for synapse dynamics,[27,28] it is not necessary for dimer formation.[29,30] From this, one can infer that the EC-region is an active player in cadherin-mediated cell−cell adhesion. Thus, critical information necessary for formation and dynamics of synapses is contained within the primary structure of the EC-region.

The EC-region comprises five tandemly repeated domains of ∼110 amino acids, which have an IgG-like structure consisting of a seven-stranded antiparallel β-barrel organized into two opposing sheets.[31] The EC-domains are numbered EC1-EC5 starting from the N-terminus. The specific binding of three calcium ions between each successive domain pair rigidifies the molecule to

Received: August 13, 2010
Revised: February 28, 2011
Published: March 04, 2011

ACS Publications © 2011 American Chemical Society

adopt an elongated, curved structure.[32−34] The structural and functional characteristics of cadherin are critically dependent upon calcium binding.[35,36] The studies in this paper focus on a simplified construct that contains only the first two domains of the extracellular regions of N- and E-cadherins, NCAD12 and ECAD12. This truncated construct has been studied extensively both structurally and functionally,[37−40] and is widely considered the minimal functional unit for dimerization of cadherins.[41]

In this present work, we characterize dimeric forms of NCAD12 that are distinguished by the kinetics of disassembly. The time scales of disassembly of these dimeric forms are similar to those reported in the literature for dynamics of dendritic spines in vivo, providing a possible link between dimeric forms of the EC-domains and spine dynamics. Our observation regarding the intrinsic difference between ECAD12 and NCAD12 shifts the focus of segregation of cadherins in tissues from the thermodynamic to the kinetic stability of adhesive interactions.

■ EXPERIMENTAL PROCEDURES

Plasmid Construction. The cDNA of mouse N-cadherin was provided by Dr. L. Shapiro (Columbia University, USA) and was used as a template for PCR amplification of the gene for the first two domains (residues 1−221), designated as NCAD12. The ECAD12 clone was provided by Dr. J. Engel (Biocenter, Basel, Switzerland) and coded for residues 1−219 of the protein from mouse epithelial cells, designated as ECAD12. PCR amplification of the two-domain fragments, digestion of template DNA with restriction enzymes, ligation of the fragments into the pET30 Xa/LIC expression vector (Novagen), and subsequent transformation into *Escherichia coli* BL21 (DE3) expression cells were performed according to standard protocols, utilizing KOD HiFi DNA Polymerase (Stratagene) and Xa/LIC cloning kit (Novagen). The full-length genes were sequenced to confirm the absence of mutations.

Expression and Purification. Protein expression and fractionation of inclusion body pellets were described previously.[42] The pellets were suspended in denaturing His Tag binding buffer (6 M urea, 20 mM Tris/HCl, 0.5 M NaCl, 5 mM imidazole, pH 7.5). Supernatants were applied to a Ni affinity column (GE LifeSciences). The protein was eluted with 10 mM Tris/HCl, 250 mM NaCl, 0.5 M imidazole, pH 7.9. The elution fractions containing ECAD12 and NCAD12 were dialyzed in 140 mM NaCl, 20 mM Tris, 5 mM $CaCl_2$, 1 mM DTT, and 5% glycerol, pH 7.4. Immobilized trypsin (Pierce) was used to remove the 45 residue N-terminal affinity label. Digested proteins were dialyzed against 140 mM NaCl and 10 mM HEPES, pH 7.4. The dialyzed proteins were further purified by size exclusion chromatography (SEC) using a Sephacyl S-100 (GE LifeSciences), 1.2 cm × 0.5 m (∼100 mL) column in 140 mM NaCl and 10 mM HEPES, pH 7.4. The residual calcium in the SEC buffer was found to be less than 1 μM by inductively coupled plasma optical emission spectroscopy.

The two proteins showed a significant difference between the elution profiles from preparative SEC. ECAD12 eluted as a single peak. All fractions containing ECAD12 were combined to make a single stock. NCAD12 eluted as two distinctive overlapping peaks. Fractions containing NCAD12 were not combined but kept separately and analyzed individually by analytical SEC to determine the monomer to dimer ratio in each. Note that the level of dimer in the NCAD12 dimer stocks was unchanged upon dilution for incubation periods of months. This stable dimer will be referred to as a "kinetically-trapped dimer".

Protein stocks were aliquotted and stored at 4 °C. All protein stocks were stored in the apo state. The extinction coefficients were determined experimentally and found to be 17700 ± 500 M^{-1} cm^{-1} for monomeric NCAD12 and 20600 ± 900 M^{-1} cm^{-1} for ECAD12 at 280 nm.[43] Purity of proteins was assessed by SDS−PAGE. Purified protein masses were confirmed by mass spectrometry (Stanford University). All further studies were performed under apo-buffer conditions (140 mM NaCl, 10 mM HEPES, pH 7.4) or calcium-added buffer conditions (1 mM calcium, 140 mM NaCl, 10 mM HEPES, pH 7.4). Since ECAD12 has a single cysteine residue, 1 mM TCEP was added to both buffers.

Calcium Binding Studies. Direct calcium titrations were performed on protein solutions at 2.5 μM concentration in 140 mM NaCl, 10 mM HEPES, pH 7.4 at 25 °C in a 0.4 × 1 cm cuvette with stirring by addition of small volumes (2, 5 or 10 μL) of calcium chloride stocks of different concentrations (1 mM, 10 mM, 100 mM and 0.7 M). After each calcium addition, spectra were taken from 220 to 300 nm with 5-s averaging time. Each titration was performed in triplicate. The spectra were corrected for offset differences. CD data at wavelengths between 227 and 235 nm were processed and analyzed as individual titration curves. The free calcium concentration was assumed to be equivalent to the total calcium concentration since the protein concentration is low. Data were fit to the following equation to resolve the free energy change of calcium binding. Baselines were fit to linear functions with adjustable slope and intercept parameters.

$$\overline{Y} = \frac{K_a[Ca^{2+}]}{1 + K_a[Ca^{2+}]}; \quad \Delta G^\circ = -RT \ln K_a \qquad (1)$$

Analytical SEC Studies. *Conditions and Calibration:* Analytical SEC was used to detect the presence of a dimer in protein stocks. These experiments were performed using an ÄKTA Purifier HPLC (GE LifeSciences) with a Superose-12 10/300 GL column (GE LifeSciences) with detection at 280 nm and 0.5 mL/min flow rate. The column volume is ∼25 mL. The total time to elute monomer was 30 min. The SEC column was calibrated with human serum albumin, ovalbumin, myoglobin and cytochrome-c as the standard proteins. Blue dextran and acetone were used to determine the excluded and total volumes, respectively. ECAD12 and NCAD12 eluted earlier than expected such that their apparent molecular weights were approximately twice that expected based on relative molecular mass; NCAD12 monomer appears to be 39 000 (M_r = 24 233), and dimer 65 000 (M_r = 48 466). The difference between their actual and apparent size is due to their elongated shapes. To account for the nonspherical shape, standard curves were revised to reflect the Stokes radii of the standard proteins. These standard curves yielded values of experimentally determined Stokes radii of the monomeric and dimeric forms of the cadherin construct. We compared these experimentally determined values to values calculated using HYDROPRO [44] (1edh.pdb[37]). Experimental and calculated values were identical, thereby confirming the identity of the peaks in the chromatograms. There was no indication of species larger than dimer in the chromatograms. Thus, no higher order oligomers or aggregates that eluted in the void volume were apparent.

Dissociation Kinetics Using Analytical SEC. In the first set of experiments, Analytical SEC was used to assess the overall differences in the kinetics of dimer disassembly in solutions of NCAD12 and ECAD12. The protein concentration was varied to control the level of dimer in the samples. The calcium concentration in the stocks was controlled such that the proteins were either apo (1 μM calcium) or saturated (1 mM calcium). The mobile phase was apo buffer. Thus, regardless of the calcium levels in the protein samples before injection, they were buffer exchanged into apo conditions on the column immediately after injection. Protein samples are necessarily diluted as they pass through the SEC column, so dimer will disassemble over the course of these experiments if it is in exchange with monomer. Analytical SEC experiments were done in two different ways to assess the monomer−dimer equilibria as a function of protein and calcium concentration. Each experiment was repeated at least three times.

Monomer−Dimer Equilibria as a Function of Protein Concentration. To monitor the monomer−dimer equilibria as a function of protein concentration, protein fractions (dilute protein stocks) from preparative SEC were injected on the analytical SEC column without any changes. These protein fractions were concentrated 5-fold in centrifugal concentrator units at 4 °C and analyzed by SEC immediately. In a second set of experiments, 1 mM calcium was added to dilute (17 μM) and concentrated (180 μM) stocks and injected on the column immediately.

Characterization of the Kinetically Trapped Dimer Species: Finally, the kinetically trapped dimer of NCAD12 was characterized by diluting dimer-enriched stocks from the preparative SEC and injecting them on the analytical SEC column within 30 min to weeks and to months of incubation after dilution at 4 °C. Injection volumes were 50−250 μL and protein concentrations ranged from 10 to 200 μM.

Determination of the Equilibrium Dimer Dissociation Constant: The fact that NCAD12 makes a kinetically trapped dimeric species allowed us to expand the chromatographic technique into a quantitative method for determining the equilibrium dissociation constant. Calcium (1 mM) was added to protein stocks of different concentrations (2.5, 5, 10, 20, 25, 40, 80, 110, and 230 μM) and incubated for overnight at 4 °C, to establish the monomer−dimer equilibrium. Since NCAD12 forms a kinetically trapped dimer upon decalcification, 5 mM EDTA was added to each sample and incubated for 40 min. The decalcified protein samples were then injected on the analytical SEC column and the level of dimer and monomer was determined. The fraction dimer, f_D, is a function of the total protein concentration, X, according to eq 2, where K_d is the equilibrium dimer dissociation constant.

$$f_D = \frac{x - (-K_d \pm \sqrt{K_d^2 + 8K_d x})/4}{x} \qquad (2)$$

Data were also fitted to a model that allowed for the presence of inactive monomer. The experiment was repeated in triplicate. Dilution of protein samples on the column will not affect the level of dimer because it is kinetically trapped and does not dissociate on the column.

Sedimentation Velocity Studies. Sedimentation velocity experiments were conducted in a Proteome Lab XL-I analytical ultracentrifuge (Beckman Coulter) following standard procedures.[45] Briefly, samples at concentrations of 1 mg/mL (40 μM) and 0.2 mg/mL (8 μM) were inserted in double-sector Epon centerpieces and centrifuged at 60 000 rpm while concentration profiles were acquired with the interference optics. Data analysis was performed with the software SEDFIT, using a sedimentation coefficient distribution model $c(s)$.[46] Peaks were integrated to determine the weighted-average sedimentation coefficients, and these data were assembled into an isotherm and analyzed in the software SEDPHAT with a dimerization model following the law of mass action.[47]

For a qualitative assessment of the kinetics of dimerization relative to the time-scale of sedimentation, Bayesian prior probabilities were applied to the regularization during the calculation of the sedimentation coefficient distributions[48] in a way that embeds the expectation of a slow exchange, where $c(s)$ peaks of the reacting mixture would coincide with those of the monomer and dimer species, s_1 and s_2, respectively. Apparent populations of species in $c(s)$ occurring in between these s-values, despite the regularization favoring the populations of s_1 and s_2, unequivocally demonstrates the presence of dimers that dissociate on the time-scale of the sedimentation experiment, and as a result have time-average s-values in between s_1 and s_2.

Theoretical sedimentation coefficients were predicted from the crystal structure (1ff5.pdb [34]) of the monomer and dimer, using the boundary element method as implemented in the software BEST kindly provided by Dr. Sergio Aragon.[49]

Thermal-Unfolding Studies. Spectra and thermal unfolding of ECAD12 and NCAD12 were monitored with AVIV 202SF circular dichroism (CD) spectrometer. Spectra were taken from 200 to 300 nm using a 0.5 mm path cuvette with 5 s averaging time at 25 °C. All thermal unfolding experiments were performed using a quartz cuvette with 1 cm path length fitted with a screw top through which the temperature probe was inserted. The temperature ramp rate was 1 °C/min with a 30 s to 1 min equilibration time with a 5 s acquisition time at a fixed wavelength between 225 to 235 nm with stirring. To observe the effect of calcium binding, studies were performed in apo- and calcium-added buffers. To confirm that protein stocks were in the apo buffer condition, experiments were performed with 50 μM EGTA added. To address whether the presence of the kinetically trapped dimer affected the unfolding transition, experiments were repeated on fractions from preparative SEC of NCAD12 that were predominantly monomer, a monomer and dimer mixture and predominantly dimer. The reversibility of the transitions was examined by recording the CD signal from cooling scans immediately after heating the samples.

The thermal-denaturation transitions were fit to the Gibbs−Helmholtz equation with linear native and denatured baselines with adjustable slopes and intercepts as described previously.[50] Unfolding transitions in the apo-state were two-state transitions. To test the sensitivity of resolved parameters to the value of ΔC_p, transitions were fit with ΔC_p fixed to 0, 4, 8, or 12 kJ/(mol·K). ΔH_m decreased by 12 kJ/mol and T_m decreased by 0.5 °C for ΔC_p values between 0 and 12 kJ/(mol·K). Thus, the values of resolved parameters were almost insensitive to the value of ΔC_p.

RESULTS

The present work characterizes the kinetically distinct dimeric species of N-cadherin as a function of solution conditions and incubation time. We first establish that NCAD12 and ECAD12 bind calcium with equal affinity. Second, we use a simple chromatographic technique to characterize the striking

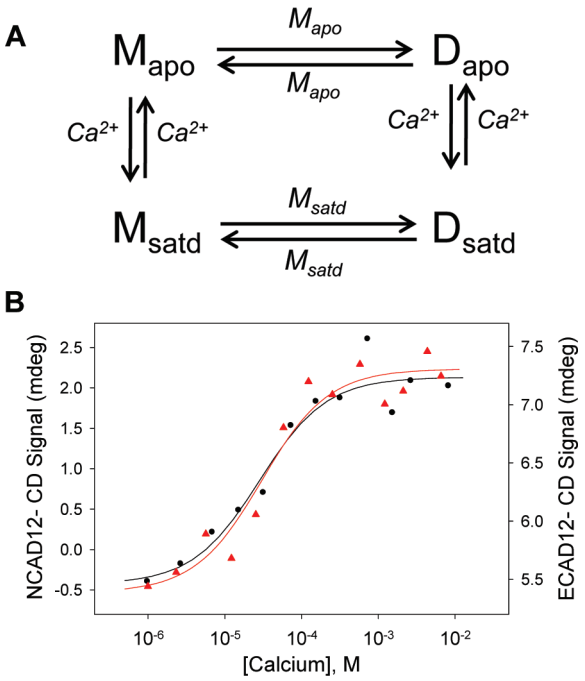

Figure 1. Linked equilibria and calcium titrations of ECAD12 and NCAD12. (A) Model showing the four-linked equilibria for the ECAD12 and NCAD12 (M_{apo} - calcium-free monomer, D_{apo} - calcium-free dimer, M_{satd} - calcium-bound monomer and D_{satd} - calcium-bound dimer). Literature values for the dimer dissociation equilibrium constant, K_d, for saturated dimers (D_{satd} to M_{satd}) is 25 μM for NCAD12 and 100 μM for ECAD12.[52] The K_d values for the dissociation of apo dimers (D_{apo} to M_{apo}) are not known. (B) Calcium titrations of NCAD12 (black) and ECAD12 (red) monitored by circular dichroism at 229 nm. Protein concentration was 2.5 μM. Solid curves were simulated based on best fit parameters to eq 1. The average resolved free energy change for three titrations of both proteins was -26 ± 1 kJ/mol.

difference in the disassembly kinetics of dimeric species that form in the absence and presence of calcium. Third, we use sedimentation velocity to characterize an additional dimeric species that, although trapped as dimer in apo conditions, is released to an exchangeable and fully functional form upon addition of calcium. Finally, we find that the most thermally stable construct, NCAD12, forms a slow dissociation dimer. These studies provide evidence that the kinetics of dimer disassembly of the extracellular domains may be a significant contributor to the morphological dynamics of synapses in vivo.

Linkage Diagram. Figure 1A illustrates the linkage between the calcium binding and dimerization equilibria. The horizontal equilibria represent dimerization in the absence of calcium (M_{apo} to D_{apo}; top) and presence of calcium (M_{satd} to D_{satd}; bottom). The vertical equilibria represent the binding of calcium to the monomeric species M_{apo} to form M_{satd} (left) and to the dimeric species D_{apo} to form D_{satd} (right). Since monomer and dimer species are in equilibrium, their relative population in solution will depend upon protein concentration. In vivo, under typical extracellular conditions, the calcium concentration is high (1−2 mM).[51] Thus, the $M_{apo}-D_{apo}$ equilibrium is not physiologically relevant, but must be considered as part of the linkage between calcium binding and dimerization. Studies in this paper address the difference in the calcium-dependent kinetics of dimer disassembly.

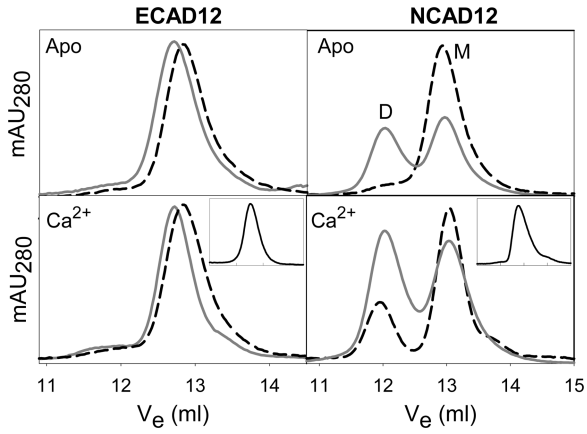

Figure 2. Analytical SEC to determine the monomer−dimer equilibria as a function of protein and calcium concentrations. Dilute NCAD12 and ECAD12 stocks (17 and 30 μM, respectively; dashed) were concentrated (180 and 100 μM, respectively; solid) in apo (1 μM calcium; top) and calcium-bound states (1 mM calcium; bottom) to show the effect of protein and calcium concentration on the monomer and dimer equilibria. These samples were analyzed under apo-buffer conditions. Insets: Calcium-saturated samples analyzed by SEC in a chromatography buffer containing 1 mM calcium. Scale is identical to the chromatograms under apo-buffer conditions.

Calcium Binding Studies. We performed calcium titrations of NCAD12 and ECAD12 in order to establish the buffer conditions under which the proteins were apo and calcium saturated. Calcium titration of apo-NCAD12 and apo-ECAD12 at low protein concentration (M_{apo} to M_{satd}) yielded transitions that were monotonic with clear apo and saturated baselines (Figure 1B). Transitions fitted to eq 1 showed random residuals with no indication of cooperativity. Analysis of binding data for the two proteins yielded identical free energy changes of -26 ± 1 kJ/mol (K_d (Ca) = 30 μM). Titrations were performed in triplicate and the standard deviation in the resolved value for the free energy change of binding was greater than the standard deviation in the average free energies. This value represents the average dissociation constant for binding of all three calcium ions at the interface between domains 1 and 2 to the monomeric species. For the purposes of the subsequent assembly studies, the proteins are in the apo-state in the low calcium buffer conditions (1 μM). In the high calcium buffer conditions (1 mM), the proteins are saturated. Thus, the calcium ligation state is controlled by the sample buffer composition.

Assembly Studies. *Monomer−Dimer Equilibria as a Function of Protein and Calcium Concentration:* The most striking difference in NCAD12 and ECAD12 is illustrated in Figure 2, where a simple chromatographic method was used to assay for the relative level of dimer in protein solutions. ECAD12 eluted as a single peak regardless of the calcium conditions, with a small protein-concentration dependent difference in the elution volume. The smaller elution volume at high protein concentration is consistent with the formation of more dimer. Thus, for ECAD12, the equilibria between M_{apo} and D_{apo} and between M_{satd} and D_{satd} are rapid on the time scale of the chromatographic experiment indicating fast association and dissociation kinetics. This is in contrast to the behavior observed for NCAD12 as discussed below.

Apo-NCAD12 eluted as two peaks indicating the slow dissociation rate of D_{apo} on the time scale of the chromatographic

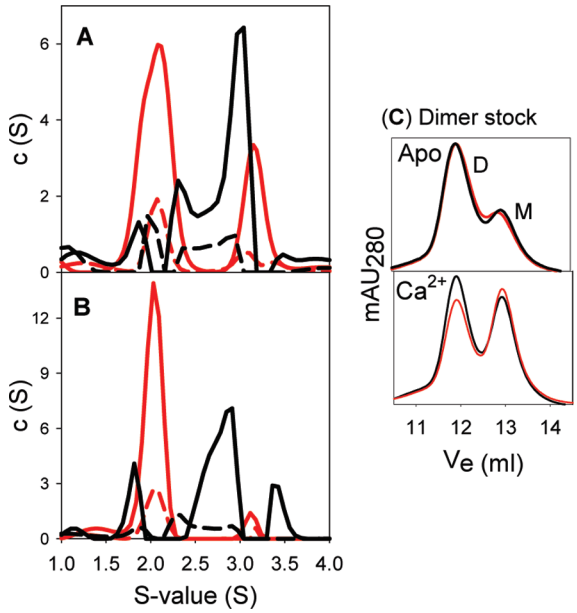

Figure 3. Characterization of kinetically trapped dimeric species of NCAD12. Sedimentation coefficient distributions $c(s)$ of NCAD12 stocks from preparative SEC enriched in (A) kinetically trapped dimer and (B) in monomer under four different experimental conditions: apo-dilute (0.2 mg/mL; red dashed), apo-concentrated (1 mg/mL; red solid), 1 mM calcium-dilute (0.2 mg/mL; black dashed), and 1 mM calcium-concentrated (1 mg/mL; black solid). (C) SEC analysis of kinetically trapped dimer enriched NCAD12 stocks from preparative SEC. Top panel shows the concentrated (black, 68% dimer) and 1 to 5 diluted (red, 68% dimer) apo-NCAD12 dimer-enriched stock. Bottom panel shows the concentrated (black, 54% dimer) and 1 to 5 diluted (red, 47% dimer) calcium bound NCAD12 dimer-enriched stock.

experiment (Figure 2). The dimer concentration increased as a function of protein concentration (Figure 2). The calcium added samples showed an increase in dimer concentration, which indicates the stronger dimerization in the presence of calcium. It is important to note that although the sample is in high calcium concentration, the assay is not. Distinct monomer and dimer peaks in these high calcium samples result from the apo-buffer used in the chromatographic analysis and slow dimer disassembly of apo protein on the chromatographic time scale. Analysis of calcium-added samples in a high calcium chromatography buffer yielded a single peak with a retention volume that depended upon the protein concentration (insets, Figure 2), thereby illustrating that D_{satd} disassembles rapidly. Thus, calcium increases the binding constant and the rate of disassembly of the dimer. In conclusion, apo-NCAD12 and ECAD12 differ significantly in the kinetics of the monomer−dimer equilibrium.

Characterization of the Kinetically Trapped Dimer. The following two experiments were performed to characterize the third dimeric form of NCAD12. This species was first observed in the preparative SEC of NCAD12 (Materials and Methods). Subsequently, we discovered that we could make this kinetically trapped dimer by decalcifying the calcium-saturated NCAD12 stocks.

Sedimentation Velocity. Sedimentation velocity (SV) analytical ultracentrifugation experiments were conducted in order to independently confirm the presence of the very slow dissociation dimer and to test its response to calcium levels. Data from the SV experiment are shown in Figure 3. Two separate fractions from the preparative SEC experiment were analyzed. One fraction had a higher abundance of the dimer (i.e., the kinetically trapped dimer) and the other fraction was predominantly monomer. Figure 3A shows the sedimentation coefficient distributions of the enriched-dimer fraction without added calcium at a concentration of 1 mg/mL (40 μM; red-solid) and after dilution to 0.2 mg/mL (8 μM; red-dashed). The extraordinary "stability" of the dimer is demonstrated by the fact that the weighted-average s-values of both samples are identical within error (2.37 S at 1 mg/mL and 2.40 S at 0.2 mg/mL), showing that there has been no rearrangement of the populations of monomer and dimer after dilution (incubated for ~2 weeks in diluted state). Further, the measured $s_{20,w}$ values of the monomer and dimer peaks (2.10 and 3.27 S, respectively) were in excellent agreement with those predicted from calculations of the translational frictional coefficient based on structural models (2.06 and 3.21 S, respectively), supporting that the monomer and dimer are essentially stable species in solution. This stable dimer is "kinetically trapped" since it is not in dynamic equilibrium with monomer.

In the presence of calcium, under otherwise identical conditions, the species re-equilibrate and exhibit concentration-dependent weighted-average s-values of 2.73 S for the concentrated enriched-dimer stock (black-solid) and 2.45 S for the diluted enriched-dimer stock (black-dashed; Figure 3A). This indicates that there is dimer present since the s-values are greater than that for monomer alone and that the dimer is in rapid exchange with monomer. The decrease in s-value in the diluted sample indicates that there is less dimer in the sample.

In order to further confirm that the trapped dimer is not an aggregate, but rather a fully functional, albeit trapped, species a second series of experiments were performed on NCAD12 monomer stocks (Figure 3B). Without calcium, the weighted-average s-values of this monomer enriched sample are 2.09 and 2.11 S at 1 mg/mL and 0.2 mg/mL, respectively. After calcium was added, under otherwise identical conditions, the values of 2.69 and 2.37 S were measured for the undiluted and diluted sample, respectively. These values are very close to those from the stock enriched in the kinetically trapped dimer as starting material (Figure 3A). The weighted-average s-values in the presence of calcium can be modeled with a binding isotherm (knowing monomer and dimer s-values, since these are measured in the conditions suppressing the exchange). This leads to estimates of K_d of 26 μM for the monomer-enriched sample and 22 μM for the dimer-enriched sample which is identical within error of measurement. This demonstrates that in the presence of calcium both the monomer-enriched and kinetically trapped dimer-enriched fractions relax to the same equilibrium. This is a critical point which illustrates that the kinetically trapped dimer is not aggregate but is a functional protein that is released from its trapped state by the addition of calcium.

Figure 3 highlights the dynamic exchange on the time-scale of sedimentation (i.e., $k_{off} > 0.001/s$) in the presence of calcium by displaying signal density in the $c(s)$ distribution at values intermediate to those of the monomer and dimer s-values. These signals are caused by dimers that during the sedimentation experiment dissociate into monomers and therefore represent a population of molecules that have an intermediate average velocity. Technically, the detection of this population was enhanced (and distinguished from broadening of $c(s)$ caused by regularization) by using the Bayesian regularization method $c^P(s)$ applied so as to account, as much as statistically permitted by the fit of the measured data, for the sedimenting species either as stable monomers or as dimers but not intermediates. The fact

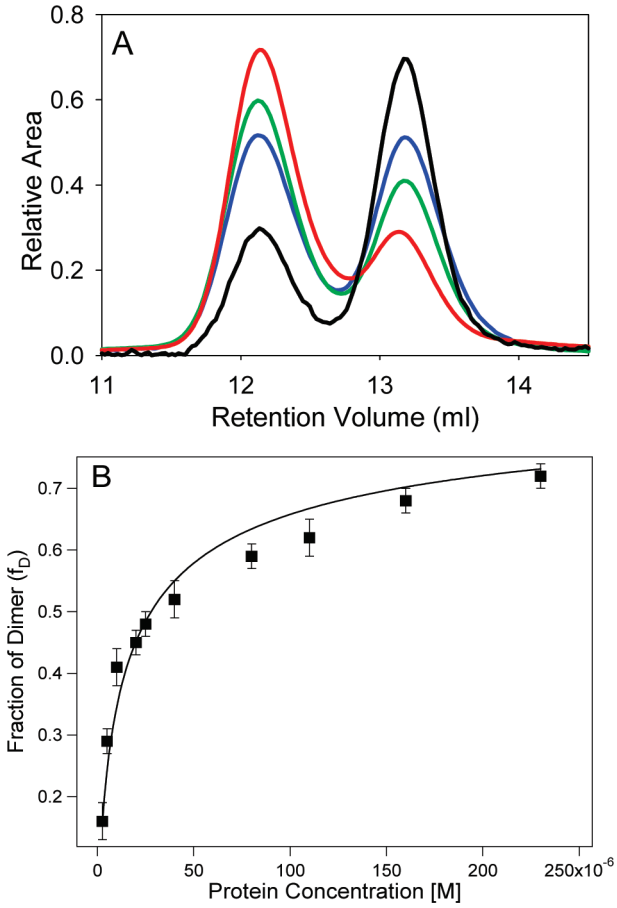

Figure 4. Determination of the equilibrium dimer dissociation constant. The analytical SEC technique was adapted to measure the equilibrium dimer dissociation constant for NCAD12. EDTA was added to form the kinetically trapped dimeric species in a set of protein solutions of differing concentrations. (A) Representative chromatograms showing D^*_{apo} (12.1 mL) and monomer (13.2 mL) over a range of protein concentrations (5 μM (black), 25 μM (blue), 110 μM (green), and 220 μM (red)). (B) Dimer fraction is plotted versus the total protein concentration. The line is simulated based on the best fit values resolved from fitting the data to eq 2.

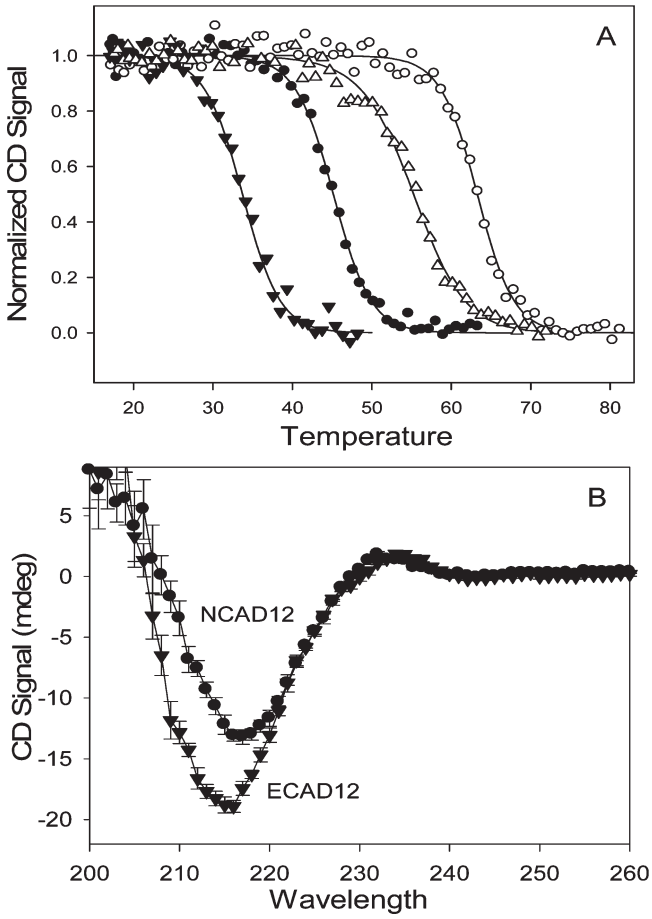

Figure 5. Thermal-denaturation of ECAD12 and NCAD12. (A) Thermal-denaturation of ECAD12 (triangles) and NCAD12 (circles) at 230 nm. Normalized CD signal versus temperature (°C) at 1 μM (filled) and 1 mM (open) calcium at 5 μM protein concentrations. (B) CD spectra of ECAD12 (triangles) and NCAD12 (circles) in the apo-state (140 mM NaCl, 10 mM HEPES, pH 7.4).

that $c^P(s)$ displays, despite this prior assumption to favor the opposite result, these intermediate signals demonstrate that they are highly significant and unequivocally reported by the measured data (see ref 48).

In analogous experiments with ECAD12 (data not shown), the population of species in the apo-state was predominantly monomeric (weighted average *s*-values of 2.11 S at 1 mg/mL and 2.06 S at 0.2 mg/mL). Addition of calcium caused a small change the *s*-values (2.33 S at 1 mg/mL and 2.03 S at 0.2 mg/mL). Thus, re-equilibration was detected via a slight increase of the s_w value. The increase in the s_w value by 0.3 S suggests dimer fractions in the 1 mg/mL sample to be between 10 and 50%, qualitatively consistent with the K_d values reported by Katsamba et al.[52] Unfortunately, the highest concentration of 1 mg/mL (40 μM) of ECAD12 did not lead to sufficiently high dimer populations, and the thermodynamics and kinetics of re-equilibration was not accessible.

Analytical SEC. Analytical SEC confirmed the existence of a kinetically trapped dimer species for NCAD12 (Figure 3C, top). When the dimer enriched sample (50 μM; black) from the preparative SEC was diluted to 10 μM (red) in low calcium buffer, the abundance of dimer was unchanged and the level of dimer was constant for up to a month after dilution, indicating that the dimer is not in equilibrium with monomer. Next, we tested whether the kinetically trapped dimer would equilibrate with monomer by adding 1 mM calcium (Figure 3C, bottom). The NCAD12 dimer concentration decreased with calcium addition, indicating that calcium released the trapped dimer (black). Upon dilution (red), the dimer dissociated, which indicates that this released dimer was in exchange with monomer. Taken together, the SEC and SV data indicate that the kinetically trapped dimer was, after calcium addition, fully equivalent in behavior to the preparative monomer fraction. Thus, the kinetically trapped dimer (D^*_{apo}) is a dimeric form that is distinguished from D_{apo} and D_{satd} since it is not in equilibrium with monomer.

Determination of the Equilibrium Dimer Dissociation Constant. As additional conformation of the viability of our NCAD12 protein stocks, and to extend the utility of the chromatographic method, we performed a series of experiments to determine the equilibrium dissociation constant for dimerization. In these experiments, solutions of known protein concentrations and 1 mM calcium concentration were prepared such that there was an equilibrium mixture of monomer and dimer

Table 1. Parameters Resolved from Thermal−Denaturation Experiments[a]

protein	buffer	ΔH_m (kJ/mol)	T_m (°C)	ΔG^o (kJ/mol)
ECAD12	apo	330 ± 40	33.7 ± 0.4	8 ± 2
ECAD12	1 mM Ca^{2+}	280 ± 20	55.2 ± 0.5	13 ± 3
NCAD12	apo	360 ± 20	45.1 ± 0.2	17 ± 2
NCAD12	1 mM Ca^{2+}	400 ± 20	63.3 ± 0.2	28 ± 3

[a] The value of ΔC_p for NCAD12 was fixed to 8.4 kJ/(mol·K), and for ECAD12 was fixed to 4.2 kJ/(mol·K). $\Delta G°$ is the calculated value of the free energy change upon unfolding at 25 °C.

(D_{satd}) as dictated by the protein concentration. EDTA was added and the calcium stripped from the dimer leading to formation of the kinetically trapped dimer. The level of D^*_{apo} was then assayed using the analytical SEC method. A representative set of chromatograms is shown in Figure 4A. There is a clear concentration-dependent trend in the level of dimer in the sample. The fraction of dimer is plotted versus the total protein concentration in Figure 4B. The data were fitted to eq 2 and yielded the K_d of 28 ± 4 μM (100% active protein). If we considered the possibility of inactive monomer, the data were fit best with a K_d of 18 ± 4 μM with 90% of the protein active. The dimer concentration increases with an increase in the protein concentration. Overall, these results confirm that the protein is active and forms dimer with a dimerization constant consistent with our sedimentation velocity experiments and with published reports.

Thermal Unfolding Studies. Results from the thermal-unfolding experiments of dilute protein solutions are summarized in Figure 5. The CD signal at 225 nm decreased as the proteins unfolded. This has been reported previously for MECAD12, a two domain construct of ECAD12 with an extra N-terminal methionine.[42] Thus, in the case of cadherin, a larger signal (more negative) indicates formation of random coil.[42,50] We draw two conclusions from these unfolding transitions. First, M_{apo} of ECAD12 is significantly less stable than M_{apo} of NCAD12. Second, both constructs are significantly stabilized by calcium. Stabilization by calcium would be expected since both constructs bind calcium.[53]

Unfolding data were fit to the Gibbs−Helmholtz equation and resolved parameters are reported in Table 1. The ΔC_p values for similar constructs have been determined experimentally to be 8 kJ/(mol·K) for apo-MECAD12 [42] and 4 kJ/(mol·K) for apo-NCAD12 (data not shown). The greater stability of apo-NCAD12 is manifested as a higher T_m when compared to ECAD12, with no observed difference in ΔH_m. Upon addition of calcium the T_m for ECAD12 increased by 22 °C, and for NCAD12 increased by 18 °C. Considering the difference in the resolved values for ΔH_m in 1 mM calcium, this represents similar stabilization by calcium for both constructs.

In order to demonstrate that the cadherin constructs are a thermodynamically tractable system, we tested the reversibility of thermal denaturation experiments. Protein solutions were heated to 90 °C, cooled back to 15 °C, equilibrated at 15 °C, and then reheated to unfold (Figure 7; Supporting Information). Refolding of apo-NCAD12 data is slow relative to the unfolding transition, but the thermal denaturation of the refolded protein was a very similar transition to the original unfolding transition. This indicates that the unfolding of the protein is reversible. The unfolding of ECAD12 was discussed elsewhere.[42]

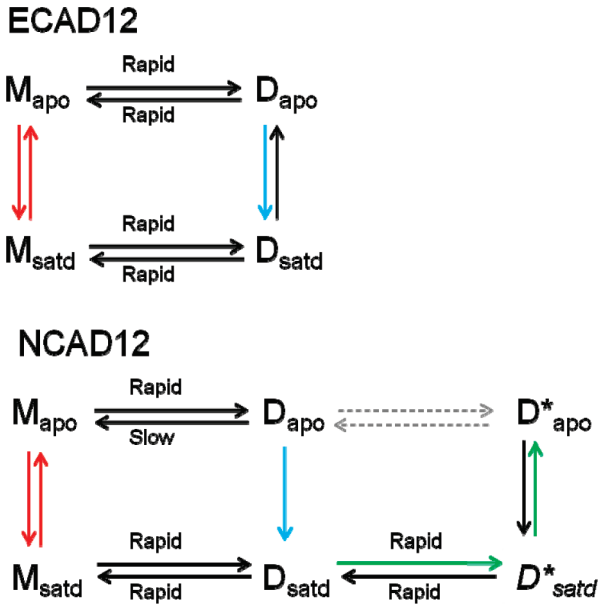

Figure 6. Exchange dynamics of monomer−dimer equilibria for ECAD12 and NCAD12. Exchange dynamics of monomer−dimer equilibrium for ECAD12 (top panel) and NCAD12 (bottom panel). Solid arrows are reactions that were observed experimentally. Calcium titrations of monomeric NCAD12 and ECAD12 are represented by solid red arrows (from Figure 1B). D_{satd} is formed through calcium addition to M_{apo}−D_{apo} stocks (blue; from Figure 2). The formation of D_{apo} depends upon the construct. For NCAD12, the green arrows represent the decalcification of D_{satd} to form D^*_{apo}. This was observed through decalcification of calcium saturated stocks on the chromatographic column or by addition of EDTA (from Figure 4). The activation energy barrier between D_{apo} and D^*_{apo} is too high to overcome without addition of heat or calcium (dashed arrows).

Thermal unfolding and reversibility experiments were also performed on kinetically trapped dimeric stocks of apo-NCAD12 in order to test whether the presence of kinetically trapped dimer would affect the apparent stability of the NACD12 stock. These studies showed that the kinetically trapped dimeric stocks have identical thermal-unfolding and reversibility profiles as monomer stocks indicating that the dimers disassemble before the proteins unfold (Figure 8; Supporting Information). The disassembly of D^*_{apo} was also observed by heating the dimer-enriched stock to 37 °C for up to 1 h and analyzing it by analytical SEC. The level of D^*_{apo} decreased with a concomitant increase in M_{apo} (data not shown).

Spectral Characterization. The CD spectra (Figure 5B) showed a wavelength minimum at approximately 218 nm as typical for β-sheet proteins.[54] Both proteins have a local maximum in the CD spectra at 235 nm, which reports 3−10 helix content and tryptophan environment.[55] This feature was very similar between the two proteins. The spectra for NCAD12 and ECAD12 differ, which indicates that the proteins have different structural asymmetry. NCAD12 showed a less negative CD signal than ECAD12 at 215 nm. Since the CD signal decreased as cadherins unfolded (Figure 5A), this difference may indicate that ECAD12 is less structured than NCAD12, correlating with the lower stability of ECAD12.

DISCUSSION

In the past decade, there has been great interest in the plasticity of excitatory synapses at dendritic spines as pertaining

to learning, memory, and disease.[56,57] Dendritic spines can change shape and contact surface on a time scale of seconds to months.[12,13] While these sorts of morphological changes are undoubtedly related to cytoplasmic factors,[58,59] we are intrigued by how the extracellular domain of N-cadherin is affected by the calcium transients that occur at an actively firing synapse. With a simple chromatographic experiment, we have studied the dimerization properties of a minimal functional unit of the extracellular domain of E- and N-cadherin to compare their dimerization properties. We have shown evidence for three distinct dimeric forms of NCAD12 which differ in the conditions of formation and the kinetics of disassembly. The exchange rates observed for these isolated extracellular domains are similar to those observed for N-cadherin in vivo. Thus, the intrinsic calcium-dependent dimerization properties of the extracellular domains of cadherins likely play a role in synaptic plasticity.

Kinetically Distinct Dimeric Forms. The analytical SEC experiments demonstrated that NCAD12 forms three different dimers that are distinguished by differences in their dissociation kinetics as a function of solution conditions. Data are summarized in the linkage diagram shown in Figure 6 (ECAD12 (top) and NCAD12 (bottom)). The M_{apo} forms of NCAD12 and ECAD12 were titrated with calcium as represented by the solid red arrows. These titration experiments demonstrated that the protein was in the apo state in the low calcium conditions of the SEC mobile phase. Additionally, they established that in 1 mM calcium, the proteins were calcium saturated. Considering dimerization equilibria of ECAD12 first, in dilute and concentrated stocks the monomeric and dimeric species are in fast exchange regardless of the calcium concentration; the equilibrium between $M_{apo}-D_{apo}$ and $M_{satd}-D_{satd}$ is rapid (solid black arrows). In summary, all ECAD12 dimers are in equilibrium with monomer regardless of the calcium concentration.

The disassembly dynamics of dimeric forms of NCAD12 differ in several ways. First, the dissociation of D_{apo} to M_{apo} is slower than seen for ECAD12. Further, the addition of calcium leads to formation of more dimer than present in the apo state (Figure 2), indicating that the dimerization constant is greater with calcium present. Finally, when a calcium-saturated NCAD12 stock is decalcified, a kinetically trapped dimer is formed (D^*_{apo}; green arrows). This D^*_{apo} is not in equilibrium with monomer upon dilution regardless of the incubation time (dashed arrows). The trapped species is released upon addition of calcium. Sedimentation velocity studies further characterized and confirmed the SEC results on the "stability" of D^*_{apo} illustrating the following major points. D^*_{apo} is a distinct species in that it sediments with a sedimentation coefficient expected for a dimer of NCAD12. Addition of calcium to the D^*_{apo} sample allowed the protein to equilibrate with monomer. In fact, the sedimentation velocity studies showed that whether the original stock was monomeric or was enriched in D^*_{apo}, they were similar after addition of calcium. This indicates that the kinetically trapped dimer is not an aggregate or misfolded protein. Calcium acts as a catalyst, lowering the activation energy barrier between D^*_{apo} and the monomeric form. This is also supported by the thermal-unfolding studies of D^*_{apo}-enriched stocks.

The three kinetically distinct dimeric species were critical to characterize in order to understand the linkage diagram (Figure 6), but are they all physiologically relevant? Since the extracellular calcium concentration is typically 1 to 2 mM,[51] it is unlikely that the D_{apo} species of ECAD12 and NCAD12 are physiologically relevant. Since the calcium concentration is typically high, the D_{satd} species would be the relevant form for most adhesions. The D^*_{apo} form of NCAD12 forms upon decalcification of solutions containing D_{satd}. It is possible that this kinetically trapped species is relevant at actively firing excitatory synapses that undergo large fluctuations in calcium concentration. There are several examples of kinetically trapped dimers from the literature. Mutant calbindin D_{9k} forms a domain-swapped dimer that is slow to assemble and disassemble, such that the dimeric species is kinetically trapped.[60] Kinetically trapped dimers were also observed in cyanovirin-N dimers under crystallization conditions.[61] Similarly, dissociation of tubulin dimer is cofactor dependent, such that the cofactors catalyze dimer dissociation.[62]

Structure and Disassembly Kinetics. There is ample evidence in the literature for hierarchical structures in cadherin assembly. These structures could give rise to the kinetically distinct dimer species reported here. An initial report of flow chamber studies by Perret et al. observed dynamics of E-cadherin complexes with a time constant of 2 s, consistent with our observations.[63] Subsequently, Perret et al. used force measurement studies to show hierarchical strengths of interactions, consistent with heterogeneity in the structure and perhaps then in the kinetics of disassembly.[64] These observations are also supported by immunoprecipitation studies by Troyanovsky et al.[29] and probe force measurements by Sivasankar et al.[65]

Recent studies on strand-crossover dimer formation of ECAD12 showed the necessity for formation of an initial encounter complex (X-dimer) in dimerization.[66] Using single molecule fluorescence resonance energy transfer, Sivasankar et al. reports an initial encounter complex with much faster assembly dynamics than a subsequent complex that forms. Later Harrison et al.[67] inferred that these complexes are important in kinetics of association and dissociation of strand-crossover dimer reporting that X-dimer formation is mediated by the interaction between amino acid residues in the β-strands and the residues near the calcium-binding sites of the adhesive partner. The residue K14 in ECAD12 forms an intermolecular salt bridge with D138 at the X-dimer interface, and disruption of this salt bridge affects the kinetics of dimerization. They show that SEC analysis of a mutant of ECAD12 (K14E) showed two peaks, which indicates slow exchange rates between monomer and dimer. Consistent with the mutant of ECAD12, NCAD12 does not have this intermolecular salt bridge (proline at position 138). Hence, the differences in the X-dimer interface between ECAD12 and NCAD12 could contribute to the difference between the dynamics of dimerization and kinetic stability of ECAD12 and NCAD12.

An alternative but complementary explanation for the differences between the D_{apo} and D^*_{apo} is found in computational studies.[68] Cailliez et al. performed a molecular dynamics study of dimeric structures that addressed, in part, the relative orientation of the monomers at the strand-crossover dimer interface. They found two distinct orientations that could be the structural basis of the kinetically distinct dimers. We also speculate that the D^*_{apo} structure may well be the form crystallized by Shapiro et al.,[69] perhaps parallel orientation of the monomers at the dimer interface.

Stability and Disassembly Kinetics. Stability studies showed that M_{apo} of NCAD12 is more stable than that of ECAD12. We believe that this increased stability of apo-NCAD12 monomer is related to the disassembly kinetics of the dimeric species. While both ECAD12 and NCAD12 are anionic proteins, ECAD12 has

significantly more negative charges at pH 7.4. Stability studies of E-cadherin as a function of salt concentration showed that electrostatic repulsion destabilizes the EC-domains.[70] We propose that the electrostatic repulsion that destabilizes the ECAD12 monomer also destabilizes the ECAD12 dimer. For these end state stabilities to affect the disassembly dynamics, it must also be true that the transition state energy is similar between NCAD12 and ECAD12. Since this energy barrier is likely related to breaking and reforming the noncovalent interactions in the strand-crossover dimer, one would expect it to be similar for the two proteins.[39,71,72] The correlation between stability and slow dimer disassembly was illustrated in another strand-swapped system, lambda Cro repressor.[73] According to those studies, increased stability of Cro F58W is correlated with slower disassembly of Cro-repressor dimers.

CONCLUSION

The molecular basis of the segregation of two members of classical cadherins, E- and N-cadherins, at synapses is not clear. E- and N-cadherins have a similar sequence and structure, and their calcium-binding residues are identical. Nonetheless, these two proteins have distinct localizations at excitatory and inhibitory synapses, where the calcium fluctuations are significantly different. Localization of these two proteins implies differences in their dimerization properties as a function of calcium. We have focused our studies on the first two domains of E- and N-cadherins, ECAD12 and NCAD12, and measured the stability and disassembly kinetics of these constructs as a function of calcium concentration. Our results showed striking differences between the dynamics of dimerization and stability of these constructs. We present evidence for three distinct dimeric forms of NCAD12 that differ by their calcium-dependent kinetics of disassembly. According to our two domain model system, N-cadherin forms a kinetically trapped dimer in the calcium-depleted environment of an excitatory synapse. Interestingly, these distinct kinetic species are mirrored in the behavior of excitatory synapses in vivo. Mysore et al. observed distinct populations of dendritic spines that displayed changes in synapse shape occurring on the time scale of minutes to hours.[13] Synapse durations of a month have been reported by Trachtenberg et al.[12] Although we know that the exchange dynamics of the extracellular domains are not the whole story, they may be a major contributor to this heterogeneity in the morphological dynamics of synapses in vivo.

ASSOCIATED CONTENT

Supporting Information. Reversibility of thermal-denaturation of NCAD12 and thermal-denaturation of monomer and dimer enriched stocks. This material is available free of charge via the Internet at http://pubs.acs.org.

AUTHOR INFORMATION

Corresponding Author

*E-mail: spedigo@olemiss.edu; phone: 1-662-915-5328; fax: 1-662-915-7300.

Funding Sources

This work was supported by Grant MCB 0950494 from the National Science Foundation.

ABBREVIATIONS USED

apo, calcium-depleted; CD, circular dichroism; DTT, dithiothreitol; EC-region, extracellular domains; ECAD12, epithelial-cadherin domains 1 and 2 (residues 1−219); EGTA, ethylene glycol tetraacetic acid; EDTA, ethylenediaminetetraacetic acid; HEPES, *N*-(2-hydroxyethyl)piperazine-*N*′-2-ethanesulfonic acid; K_d, equilibrium dimer dissociation constant; MECAD12, E-cadherin domains 1 and 2 (res. 1−219) with extra N-terminal methionine; NCAD12, neural-cadherin domains 1 and 2 (residues 1−221); SDS−PAGE, sodium dodecylsulfate polyacrylamide gel electrophoresis; SEC, size exclusion chromatography; satd, calcium-saturated; SV, sedimentation velocity; TCEP, Tris(2-carboxyethyl)phosphine; Tris, Tris(hydroxymethyl)aminomethane

REFERENCES

(1) Shapiro, L., Love, J., and Colman, D. R. (2007) Adhesion molecules in the nervous system: structural insights into function and diversity. *Annu. Rev. Neurosci. 30*, 451–474.

(2) Yu, X., and Malenka, R. C. (2004) Multiple functions for the cadherin/catenin complex during neuronal development. *Neuropharmacology 47*, 779–786.

(3) Jungling, K., Eulenburg, V., Moore, R., Kemler, R., Lessmann, V., and Gottmann, K. (2006) N-cadherin transsynaptically regulates short-term plasticity at glutamatergic synapses in embryonic stem cell-derived neurons. *J. Neurosci. 26*, 6968–6978.

(4) Huntley, G. W., Gil, O., and Bozdagi, O. (2002) The cadherin family of cell adhesion molecules: multiple roles in synaptic plasticity. *Neuroscientist 8*, 221–233.

(5) Bekirov, I. H., Needleman, L. A., Zhang, W., and Benson, D. L. (2002) Identification and localization of multiple classic cadherins in developing rat limbic system. *Neuroscience 115*, 213–227.

(6) Redies, C. (2000) Cadherins in the central nervous system. *Prog Neurobiol. 61*, 611–648.

(7) Hirano, S., Suzuki, S. T., and Redies, C. (2003) The cadherin superfamily in neural development: diversity, function and interaction with other molecules. *Front Biosci. 8*, d306–355.

(8) Bozdagi, O., Shan, W., Tanaka, H., Benson, D. L., and Huntley, G. W. (2000) Increasing numbers of synaptic puncta during late-phase LTP: N-cadherin is synthesized, recruited to synaptic sites, and required for potentiation. *Neuron 28*, 245–259.

(9) Fannon, A. M., and Colman, D. R. (1996) A model for central synaptic junctional complex formation based on the differential adhesive specificities of the cadherins. *Neuron 17*, 423–434.

(10) Manabe, T., Togashi, H., Uchida, N., Suzuki, S. C., Hayakawa, Y., Yamamoto, M., Yoda, H., Miyakawa, T., Takeichi, M., and Chisaka, O. (2000) Loss of cadherin-11 adhesion receptor enhances plastic changes in hippocampal synapses and modifies behavioral responses. *Mol. Cell. Neurosci. 15*, 534–546.

(11) Rusakov, D. A., and Fine, A. (2003) Extracellular Ca2+ depletion contributes to fast activity-dependent modulation of synaptic transmission in the brain. *Neuron 37*, 287–297.

(12) Trachtenberg, J. T., Chen, B. E., Knott, G. W., Feng, G., Sanes, J. R., Welker, E., and Svoboda, K. (2002) Long-term in vivo imaging of experience-dependent synaptic plasticity in adult cortex. *Nature 420*, 788–794.

(13) Mysore, S. P., Tai, C. Y., and Schuman, E. M. (2007) Effects of N-cadherin disruption on spine morphological dynamics. *Front Cell Neurosci. 1*, 1.

(14) Okada, D., Ozawa, F., and Inokuchi, K. (2009) Input-specific spine entry of soma-derived Vesl-1S protein conforms to synaptic tagging. *Science 324*, 904–909.

(15) Mendez, P., De Roo, M., Poglia, L., Klauser, P., and Muller, D. (2010) N-cadherin mediates plasticity-induced long-term spine stabilization. *J. Cell Biol. 189*, 589–600.

(16) Fujiyama, F., Stephenson, F. A., and Bolam, J. P. (2002) Synaptic localization of GABA(A) receptor subunits in the substantia nigra of the rat: effects of quinolinic acid lesions of the striatum. *Eur J Neurosci. 15*, 1961–1975.

(17) Hafidi, A., and Hillman, D. E. (1997) Distribution of glutamate receptors GluR 2/3 and NR1 in the developing rat cerebellum. *Neuroscience 81*, 427–436.

(18) Knott, G. W., Quairiaux, C., Genoud, C., and Welker, E. (2002) Formation of dendritic spines with GABAergic synapses induced by whisker stimulation in adult mice. *Neuron 34*, 265–273.

(19) Yagi, T., and Takeichi, M. (2000) Cadherin superfamily genes: functions, genomic organization, and neurologic diversity. *Genes Dev. 14*, 1169–1180.

(20) Angst, B. D., Marcozzi, C., and Magee, A. I. (2001) The cadherin superfamily: diversity in form and function. *J. Cell Sci. 114*, 629–641.

(21) Nollet, F., Kools, P., and van Roy, F. (2000) Phylogenetic analysis of the cadherin superfamily allows identification of six major subfamilies besides several solitary members. *J. Mol. Biol. 299*, 551–572.

(22) Posy, S., Shapiro, L., and Honig, B. (2008) Sequence and structural determinants of strand swapping in cadherin domains: do all cadherins bind through the same adhesive interface?. *J. Mol. Biol. 378*, 952–966.

(23) Koch, A. W., Manzur, K. L., and Shan, W. (2004) Structure-based models of cadherin-mediated cell adhesion: the evolution continues. *Cell. Mol. Life Sci. 61*, 1884–1895.

(24) Heupel, W. M., Baumgartner, W., Laymann, B., Drenckhahn, D., and Golenhofen, N. (2008) Different Ca2+ affinities and functional implications of the two synaptic adhesion molecules cadherin-11 and N-cadherin. *Mol. Cell Neurosci. 37*, 548–558.

(25) Takeichi, M. (1990) Cadherins: a molecular family important in selective cell-cell adhesion. *Annu. Rev. Biochem. 59*, 237–252.

(26) Chitaev, N. A., and Troyanovsky, S. M. (1998) Adhesive but not lateral E-cadherin complexes require calcium and catenins for their formation. *J. Cell Biol. 142*, 837–846.

(27) Takeichi, M., and Abe, K. (2005) Synaptic contact dynamics controlled by cadherin and catenins. *Trends Cell Biol. 15*, 216–221.

(28) Takeichi, M. (2007) The cadherin superfamily in neuronal connections and interactions. *Nat. Rev. Neurosci. 8*, 11–20.

(29) Troyanovsky, R. B., Laur, O., and Troyanovsky, S. M. (2007) Stable and unstable cadherin dimers: mechanisms of formation and roles in cell adhesion. *Mol. Biol. Cell 18*, 4343–4352.

(30) Ozawa, M. (2002) Lateral dimerization of the E-cadherin extracellular domain is necessary but not sufficient for adhesive activity. *J. Biol. Chem. 277*, 19600–19608.

(31) Chothia, C., and Jones, E. Y. (1997) The molecular structure of cell adhesion molecules. *Annu. Rev. Biochem. 66*, 823–862.

(32) Parisini, E., Higgins, J. M., Liu, J. H., Brenner, M. B., and Wang, J. H. (2007) The crystal structure of human E-cadherin domains 1 and 2, and comparison with other cadherins in the context of adhesion mechanism. *J. Mol. Biol. 373*, 401–411.

(33) Boggon, T. J., Murray, J., Chappuis-Flament, S., Wong, E., Gumbiner, B. M., and Shapiro, L. (2002) C-cadherin ectodomain structure and implications for cell adhesion mechanisms. *Science 296*, 1308–1313.

(34) Pertz, O., Bozic, D., Koch, A. W., Fauser, C., Brancaccio, A., and Engel, J. (1999) A new crystal structure, Ca2+ dependence and mutational analysis reveal molecular details of E-cadherin homoassociation. *EMBO J. 18*, 1738–1747.

(35) Ringwald, M., Schuh, R., Vestweber, D., Eistetter, H., Lottspeich, F., Engel, J., Dolz, R., Jahnig, F., Epplen, J., and Mayer, S. (1987) et al. The structure of cell adhesion molecule uvomorulin. Insights into the molecular mechanism of Ca2+-dependent cell adhesion. *EMBO J. 6*, 3647–3653.

(36) Ozawa, M., Engel, J., and Kemler, R. (1990) Single amino acid substitutions in one Ca2+ binding site of uvomorulin abolish the adhesive function. *Cell 63*, 1033–1038.

(37) Nagar, B., Overduin, M., Ikura, M., and Rini, J. M. (1996) Structural basis of calcium-induced E-cadherin rigidification and dimerization. *Nature 380*, 360–364.

(38) Haussinger, D., Ahrens, T., Sass, H. J., Pertz, O., Engel, J., and Grzesiek, S. (2002) Calcium-dependent homoassociation of E-cadherin by NMR spectroscopy: changes in mobility, conformation and mapping of contact regions. *J. Mol. Biol. 324*, 823–839.

(39) Harrison, O. J., Corps, E. M., and Kilshaw, P. J. (2005) Cadherin adhesion depends on a salt bridge at the N-terminus. *J. Cell Sci. 118*, 4123–4130.

(40) Troyanovsky, R. B., Sokolov, E., and Troyanovsky, S. M. (2003) Adhesive and lateral E-cadherin dimers are mediated by the same interface. *Mol. Cell. Biol. 23*, 7965–7972.

(41) Shan, W., Yagita, Y., Wang, Z., Koch, A., Svenningsen, A. F., Gruzglin, E., Pedraza, L., and Colman, D. R. (2004) The minimal essential unit for cadherin-mediated intercellular adhesion comprises extracellular domains 1 and 2. *J. Biol. Chem. 279*, 55914–55923.

(42) Prasad, A., and Pedigo, S. (2005) Calcium-dependent Stability Studies of Domains 1 and 2 of Epithelial Cadherin. *Biochemistry 44*, 13692–13701.

(43) Pace, C. N., Vajdos, F., Fee, L., Grimsley, G., and Gray, T. (1995) How to measure and predict the molar extinction coefficient of a protein. *Protein Sci. 4*, 2411–2423.

(44) Garcia De La Torre, J., Huertas, M. L., and Carrasco, B. (2000) Calculation of hydrodynamic properties of globular proteins from their atomic-level structure. *Biophys. J. 78*, 719–730.

(45) Brown, P. H., Balbo, A., and Schuck, P. (2008) Characterizing protein-protein interactions by sedimentation velocity analytical ultracentrifugation. *Current Protocols in Immunology*, Wiley, New York, Chapter 18, Unit 18 15.

(46) Schuck, P. (2000) Size-distribution analysis of macromolecules by sedimentation velocity ultracentrifugation and lamm equation modeling. *Biophys. J. 78*, 1606–1619.

(47) Schuck, P. (2003) On the analysis of protein self-association by sedimentation velocity analytical ultracentrifugation. *Anal. Biochem. 320*, 104–124.

(48) Brown, P. H., Balbo, A., and Schuck, P. (2007) Using prior knowledge in the determination of macromolecular size-distributions by analytical ultracentrifugation. *Biomacromolecules 8*, 2011–2024.

(49) Aragon, S., and Hahn, D. K. (2006) Precise boundary element computation of protein transport properties: Diffusion tensors, specific volume, and hydration. *Biophys. J. 91*, 1591–1603.

(50) Prasad, A., Housley, N. A., and Pedigo, S. (2004) Thermodynamic stability of domain 2 of epithelial cadherin. *Biochemistry 43* 8055–8066.

(51) Brown, E. M., Vassilev, P. M., and Hebert, S. C. (1995) Calcium ions as extracellular messengers. *Cell 83*, 679–682.

(52) Katsamba, P., Carroll, K., Ahlsen, G., Bahna, F., Vendome, J., Posy, S., Rajebhosale, M., Price, S., Jessell, T. M., Ben-Shaul, A., Shapiro, L., and Honig, B. H. (2009) Linking molecular affinity and cellular specificity in cadherin-mediated adhesion. *Proc. Natl. Acad. Sci. U. S. A.106*, 11594–11599.

(53) Schellman, J. A. (1975) Macromolecular Binding. *Biopolymers 14*, 999–1018.

(54) Venyaminov, S. Y., and Yang, J. T. (1996) in *Circular Dichroism and the Conformational Analysis of Biomolecules* (Fasman, G. D., Ed.) pp 69−107, Plenum Press, New York.

(55) Woody, R. W., and Dunker, A. K. (1996) in *Circular Dichroism and the Conformational Analysis of Biomolecules* (Fasman, G. D., Ed.) pp 109−157, Plenum Press, New York.

(56) Tai, C. Y., Kim, S. A., and Schuman, E. M. (2008) Cadherins and synaptic plasticity. *Curr. Opin. Cell Biol. 20*, 567–575.

(57) van Spronsen, M., and Hoogenraad, C. C. (2010) Synapse pathology in psychiatric and neurologic disease. *Curr. Neurol. Neurosci. Rep. 10*, 207–214.

(58) Bamji, S. X. (2005) Cadherins: actin with the cytoskeleton to form synapses. *Neuron 47*, 175–178.

(59) Kwiatkowski, A. V., Weis, W. I., and Nelson, W. J. (2007) Catenins: playing both sides of the synapse. *Curr. Opin. Cell Biol. 19*, 551–556.

(60) Hakansson, M., Svensson, A., Fast, J., and Linse, S. (2001) An extended hydrophobic core induces EF-hand swapping. *Protein Sci. 10*, 927–933.

(61) Barrientos, L. G., Louis, J. M., Botos, I., Mori, T., Han, Z., O'Keefe, B. R., Boyd, M. R., Wlodawer, A., and Gronenborn, A. M. (2002) The domain-swapped dimer of cyanovirin-N is in a metastable folded state: reconciliation of X-ray and NMR structures. *Structure 10*, 673–686.

(62) Caplow, M., and Fee, L. (2002) Dissociation of the tubulin dimer is extremely slow, thermodynamically very unfavorable, and reversible in the absence of an energy source. *Mol. Biol. Cell 13*, 2120–2131.

(63) Perret, E., Benoliel, A. M., Nassoy, P., Pierres, A., Delmas, V., Thiery, J. P., Bongrand, P., and Feracci, H. (2002) Fast dissociation kinetics between individual E-cadherin fragments revealed by flow chamber analysis. *EMBO J. 21*, 2537–2546.

(64) Perret, E., Leung, A., Feracci, H., and Evans, E. (2004) Trans-bonded pairs of E-cadherin exhibit a remarkable hierarchy of mechanical strengths. *Proc. Natl. Acad. Sci. U. S. A. 101*, 16472–16477.

(65) Sivasankar, S., Gumbiner, B., and Leckband, D. (2001) Direct measurements of multiple adhesive alignments and unbinding trajectories between cadherin extracellular domains. *Biophys. J. 80*, 1758–1768.

(66) Sivasankar, S., Zhang, Y., Nelson, W. J., and Chu, S. (2009) Characterizing the initial encounter complex in cadherin adhesion. *Structure 17*, 1075–1081.

(67) Harrison, O. J., Bahna, F., Katsamba, P. S., Jin, X., Brasch, J., Vendome, J., Ahlsen, G., Carroll, K. J., Price, S. R., Honig, B., and Shapiro, L. (2010) Two-step adhesive binding by classical cadherins. *Nat. Struct. Mol. Biol. 17*, 348–357.

(68) Cailliez, F., and Lavery, R. (2006) Dynamics and stability of E-cadherin dimers. *Biophys. J. 91*, 3964–3971.

(69) Shapiro, L., Fannon, A. M., Kwong, P. D., Thompson, A., Lehmann, M. S., Grubel, G., Legrand, J. F., Als-Nielsen, J., Colman, D. R., and Hendrickson, W. A. (1995) Structural basis of cell-cell adhesion by cadherins [see comments]. *Nature 374*, 327–337.

(70) Prasad, A., Zhao, H., Rutherford, J. M., Housley, N. A., Nichols, C., and Pedigo, S. (2006) Effect of linker segments upon the stability of Epithelial-Cadherin Domain 2. *Proteins 62*, 111–121.

(71) Chen, C. P., Posy, S., Ben-Shaul, A., Shapiro, L., and Honig, B. H. (2005) Specificity of cell-cell adhesion by classical cadherins: Critical role for low-affinity dimerization through beta-strand swapping. *Proc. Natl. Acad. Sci. U. S. A. 102*, 8531–8536.

(72) Harrison, O. J., Corps, E. M., Berge, T., and Kilshaw, P. J. (2005) The mechanism of cell adhesion by classical cadherins: the role of domain 1. *J. Cell Sci. 118*, 711–721.

(73) Jia, H., Satumba, W. J., Bidwell, G. L., 3rd, and Mossing, M. C. (2005) Slow assembly and disassembly of lambda Cro repressor dimers. *J. Mol. Biol. 350*, 919–929.